An efficient algorithm for wave propagation in dynamic 3D configurations

M. J. Fernandes[1] S. C. Hawkins[2]

(Received 20 February 2025; revised 15 October 2025)

Abstract

We consider a model problem in which the motion of particles is examined using data carried by waves interacting with the particles. Such problems arise, for example, when tracer particles are carried by a fluid, and their position is detected using scattered light or sound waves. The time evolution of the model can be revealed by simulating the detected wave at a series of snapshots in time as their motion evolves, akin to a motion picture. In our model problem, for proof of concept, the motion of the particles is described by a simple second order ordinary differential equation, but the wave propagation simulation is extremely challenging because the governing partial differential equation must be solved in an unbounded region subject to boundary conditions on the particle boundaries, which change position as the motion of the particles evolves. The principal aim of this work is to

DOI:10.21914/anziamproc.v66.19626, © Austral. Mathematical Soc. 2025. Published 2025-12-08, as part of the Proceedings of the 22nd Biennial Computational Techniques and Applications Conference. ISSN 1445-8810. (Print two pages per sheet of paper.) Copies of this article must not be made otherwise available on the internet; instead link directly to the DOI for this article.

demonstrate the use of a fast surrogate for the solution of the wave propagation partial differential equation, and we demonstrate both the accuracy of the surrogate and its efficiency. The efficiency is crucial to allow the simulation of the wave propagation to keep up with the frame rate of the simulation.

Contents

1 Introduction

We consider fast simulation of waves scattered by particles in 3D space. This is motivated by practical applications in which information about the positions of the particles can be inferred from the wave field produced when the particles interact with an illuminating incident wave. For example, the velocity field of a fluid is revealed by tracer particles whose positions are obtained using wave scattering data. To understand the time evolution of the system, we aim to simulate the detected wave at a series of equally spaced time-steps, or frames.

When the wave speed is much faster than the speed at which the particles are moving, the wave propagation is modelled by the 3D Helmholtz equation, subject to boundary conditions that apply on the particle boundaries. Simulating the wave propagation at each frame by solving the Helmholtz PDE using traditional numerical methods is computationally expensive and the model cannot be simulated in real-time at the desired frame rate. We present

an efficient surrogate for the wave propagation model that approximates the solution of the PDE accurately and in significantly reduced time, so that real-time simulation is feasible.

Scattering problems of this type, involving the Helmholtz equation posed on an unbounded domain exterior to a number of scatterers, are commonly solved by reformulating the PDE as a surface integral equation [5] which can be solved numerically using boundary element methods [1] or mesh-free high order algorithms [9]. Alternatively, the scattering behaviour of individual scatterers can be encapsulated in the T-matrix [15, 11], and multiple scattering interactions computed by solving large linear systems based on the translation-addition theorem [7, 14]. Because the T-matrix is computed off-line and is independent of translation of the scatterers, the T-matrix approach is particularly efficient when the scattered field is required for several different configurations of the scatterers.

Despite the efficiency of the T-matrix approach, numerical results in Section 4 using the TMATROM3 package [11] for the T-matrix calculations show that this approach is too slow for real-time simulation. In this work we focus on computing the so-called far field, which describes the scattered field far away from the scatterers. We avoid full simulation of the Helmholtz PDE by considering the scatterer positions as parameters, and approximating the far field using a hybrid asymptotic/numerical approach.

The hybrid asymptotic/numerical approach has been widely applied for solution of high-frequency scattering problems using integral equations [4, 3, 6, 10]. In general, the aim is to approximate the unknown surface density in the integral equation as a product of a known highly-oscillatory function (which is derived from asymptotic results for the limit as the wavenumber goes to infinity) and an unknown slowly varying function that is amenable to numerical approximation.

The asymptotic foundation for our hybrid asymptotic/numerical approach is most closely related to early work on high-frequency multiple scattering that approximates the far field by first expressing the scattered wave as

a series, known as the Born series, whose terms describe successive order reflections between the scatterers [2]. Each term is amenable to a hybrid asymptotic/numerical approximation. Analogous approaches have been used in the integral equation context for high frequency scattering from convex scatterers [12, 8]. The novelty of this work is that we express the far field of the Born series representation of the scattered wave as a function of scatterer positions, with hybrid asymptotic/numerical approximation of series terms by products of known highly oscillatory functions and unknown slowly varying functions. We use low-degree tensor-product polynomials to approximate the slowly varying functions.

The article is structured as follows. We describe the model problem in Section 2 and our hybrid asymptotic/numerical approach in detail in Section 3. Numerical results in Section 4 demonstrate the efficiency of this approach for producing approximations that are visually accurate.

2 Problem description

Our model problem has two spherical particles situated in a closed and bounded region of $\mathbb{R}^3$, suspended from light, elastic strings fixed at $\mathbf{x}_0 \in \mathbb{R}^3$ and in motion under gravity subject to air resistance. We denote by $\mathbf{x}_j(t) \in \mathbb{R}^3$ the centre of particle $j = 1, 2$ at time $t \geq 0$, and denote by $D_j(t) \subset \mathbb{R}^3$ the region occupied by the particle. The particles have masses m_j and radii r_j. From Newton's Second Law, the motion of particle j is described by

$$m_j \ddot{\mathbf{x}}_j = m_j \mathbf{g} - \mu_j |\dot{\mathbf{x}}_j| \dot{\mathbf{x}}_j - \kappa_j \max(|\mathbf{x}_j - \mathbf{x}_0| - l_j, 0) \frac{\mathbf{x}_j - \mathbf{x}_0}{|\mathbf{x}_j - \mathbf{x}_0|}, \quad j = 1, 2, \quad (1)$$

with acceleration due to gravity $\mathbf{g}$, drag coefficients μ_j, and tension in the elastic string a function of string length l_j and string constant κ_j. The motion of the two particles is not coupled in this model, but coupling presents no difficulties for our approach.

We solve the ODE (1) using the Runge–Kutta 5(4) method to numerically approximate the position of the two particles at each frame. Figure 1 visu-

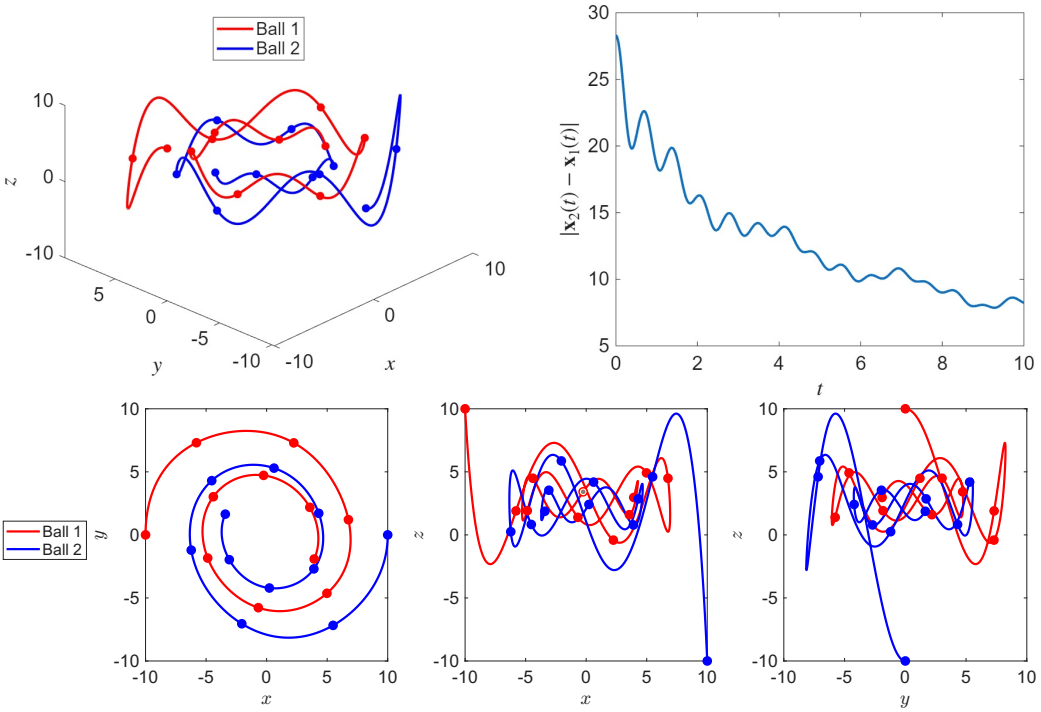

Figure 1: Trajectory of the particle centres $\mathbf{x}_1(t)$ and $\mathbf{x}_2(t)$ for $t \in [0, 20]$ with parameters given in Table 1 and initial conditions (17).

alises the motion of the particles for particular parameter values and initial conditions listed in Section 4 (Table 1, equation (17)).

At some time $t = t_f$, the region occupied by both particles is $D(t_f) = D_1(t_f) \cup D_2(t_f)$. The particles are illuminated by a time-harmonic acoustic wave with angular frequency $\omega > 0$ and wave speed c. We assume that the wave speed significantly exceeds the speed of the particles, that is, $c \gg |\dot{\mathbf{x}}_j|$ for $j = 1, 2$. The propagation of the waves outside the particles is then governed by the Helmholtz equation [5]

$$\Delta u(\mathbf{x}) + k^2 u(\mathbf{x}) = 0, \quad \mathbf{x} \in \mathbb{R}^3 \setminus \overline{D(t_f)}, \tag{2}$$

where $k = \omega/c$ is the wave number. The most interesting case for simulations, which we consider here, is when $ka \sim 1$, where a is the diameter of a scatterer.

In our simulations the particles are illuminated by an incident plane wave,

$$u^{\mathrm{inc}}(x) = e^{ikx\cdot\hat{d}}, \quad x \in \mathbb{R}^3 \setminus \overline{D(t_f)}, \tag{3}$$

with direction given by the unit vector $\hat{\mathbf{d}}$. Interaction of the incident wave with the particles induces a scattered wave $u^{\mathrm{sca}}(x)$, which also satisfies the Helmholtz equation (2), together with the Sommerfeld radiation condition [5]. For sound-soft particles, the total wave, $u^{\mathrm{tot}}(x) = u^{\mathrm{inc}}(x) + u^{\mathrm{sca}}(x)$ vanishes on the particle boundaries, so that the scattered wave satisfies the boundary conditions

$$u^{\mathrm{sca}}(x) = -u^{\mathrm{inc}}(x), \quad x \in \partial D_j(t_f), \quad j = 1, 2. \tag{4}$$

The asymptotic behaviour of the scattered wave as $|x| \to \infty$ is described by the far field

$$\psi(\hat{x}) = \lim_{|x|\to\infty} |x| e^{-ik|x|} u^{\mathrm{sca}}(x), \quad \hat{x} = x/|x|.$$

The T-matrix package TMATROM3 [11] is used to compute the far field accurately, at the expense of solving a large linear system.

3 Surrogate for the far field

For brevity we fix $t = t_f$ and omit t in our notation. We are interested in fast and accurate approximations of the far field at some fixed observation direction, $\hat{x}$, for any particle centres x_1, x_2 in $R = [-10, 10]^3 \subset \mathbb{R}^3$. Because our focus is on the behaviour of ψ with respect to the particle centres x_1, x_2 we fix the far field observation direction $\hat{x}$ and the incident wave direction $\hat{\mathbf{d}}$ and further simplify our notation by writing $\psi(x_1, x_2)$ for the far field.

We decompose the far field $\psi = \psi_1 + \psi_2$, where ψ_j is the far field radiating

from scatterer j. Each ψ_j can in turn be decomposed as

$$\psi_j = \sum_{n=0}^{\infty} \psi_j^n, \quad j = 1, 2, \tag{5}$$

where ψ_j^n is the far field radiated from scatterer j after precisely n inter-reflections between the particles. The series (5) is known as the Born series and we say the order of the term ψ_j^n is n.

Typically the terms of the Born series decay when the particles are sufficiently well separated, ensuring convergence of the series. In the numerical results in Section 4, we demonstrate that for the dynamic configurations we consider, the decay rate is sufficient that we obtain satisfactory results using just the order one approximation

$$\psi_j \approx \psi_j^0 + \psi_j^1, \quad j = 1, 2. \tag{6}$$

Next we develop approximations to the zeroth order terms ψ_j^0 and the first order terms ψ_j^1 using the following theorem, which describes the effects of translation of a particle, or particles, on its far field.

Theorem 1 (Colton and Kress [5, pp. 141–142])**.** *Let the bounded closed domain occupied by particles be* D*. For the shifted domain* $D_h = \{x + h : x \in D\}$*,* $h \in \mathbb{R}^3$*, the wave scattered by* D_h *for the incident plane wave* (3) *is*

$$u^{sca}(x; h) = e^{ikh\cdot\hat{d}}\, u^{sca}(x - h; 0), \quad x \in \mathbb{R}^3 \backslash D_h,$$

where $u^{sca}(x; 0)$ *is the wave scattered by* $D_0 = D$*. The far field of* $u^{sca}(x; h)$ *is*

$$\psi(\hat{x}; h) = e^{ikh\cdot\hat{d}} \times e^{ikh\cdot(-\hat{x})} \times \psi(\hat{x}; 0) = e^{ikh\cdot(\hat{d}-\hat{x})}\, \psi(\hat{x}; 0), \tag{7}$$

where $\psi(\hat{x}; 0)$ *is the far field of* $u^{sca}(x; 0)$*.*

Zeroth order terms Each term ψ_j^0 only depends on the position of scatterer j because no reflections are involved. From (7) with $h = x_j$,

$$\psi_j^0(x_j) = e^{ikx_j\cdot(\widehat{d}-\widehat{x})}\psi_j^0(0)\,, \quad j = 1,2\,, \tag{8}$$

and we omit $\widehat{x}$ from our notation because we consider $\widehat{x}$ to be fixed. Note that $\psi_j^0(0)$ is a constant.

First order terms For each fixed x_1, x_2, we define

$$t = \tfrac{1}{2}(x_1 + x_2)\,, \tag{9}$$

and then we view both scatterers as being translated by t from centres x_1^*, x_2^*, that is,

$$x_j = x_j^* + t\,, \quad j = 1,2\,. \tag{10}$$

Then by (7),

$$\psi_j^1(x_1,x_2) = e^{ikt\cdot\widehat{d}} \times e^{ikt\cdot(-\widehat{x})} \times \psi_j^1(x_1^*,x_2^*)\,, \quad j = 1,2\,. \tag{11}$$

From (9)–(10), $x_1^* = -x_2^*$, and so $\psi_j^1(x_1^*,x_2^*) = \psi_j^1(x_1^*,-x_1^*)$. Thus, in particular, $\psi_j^1(x_1^*,x_2^*)$ is a function of x_1^* only and so may be expressed as a function of only three variables. It is convenient to define

$$c = x_2 - x_1 = x_2^* - x_1^* = -2x_1^*\,, \tag{12}$$

and accordingly write $\psi_j^1(x_1^*,x_2^*) = \varphi_j(c)$ for some φ_j. Next we write

$$\varphi_j(c) = e^{ikx_{\neq j}^*\cdot\widehat{d}} \times e^{ik|c|} \times e^{ikx_j^*\cdot(-\widehat{x})} \times A_j^1(c)\,, \quad j = 1,2\,. \tag{13}$$

Here $e^{ikx_{\neq j}^*\cdot\widehat{d}}$ is a phase term associated with the incident wave interacting with particle $3-j$, $e^{ik|c|}$ is a phase term associated with the wave that travels from particle 1 to particle 2 or vice versa, and $e^{ikx_j^*\cdot(-\widehat{x})}$ is a phase term associated with the far field. Numerical results in Figure 2 show that the resulting

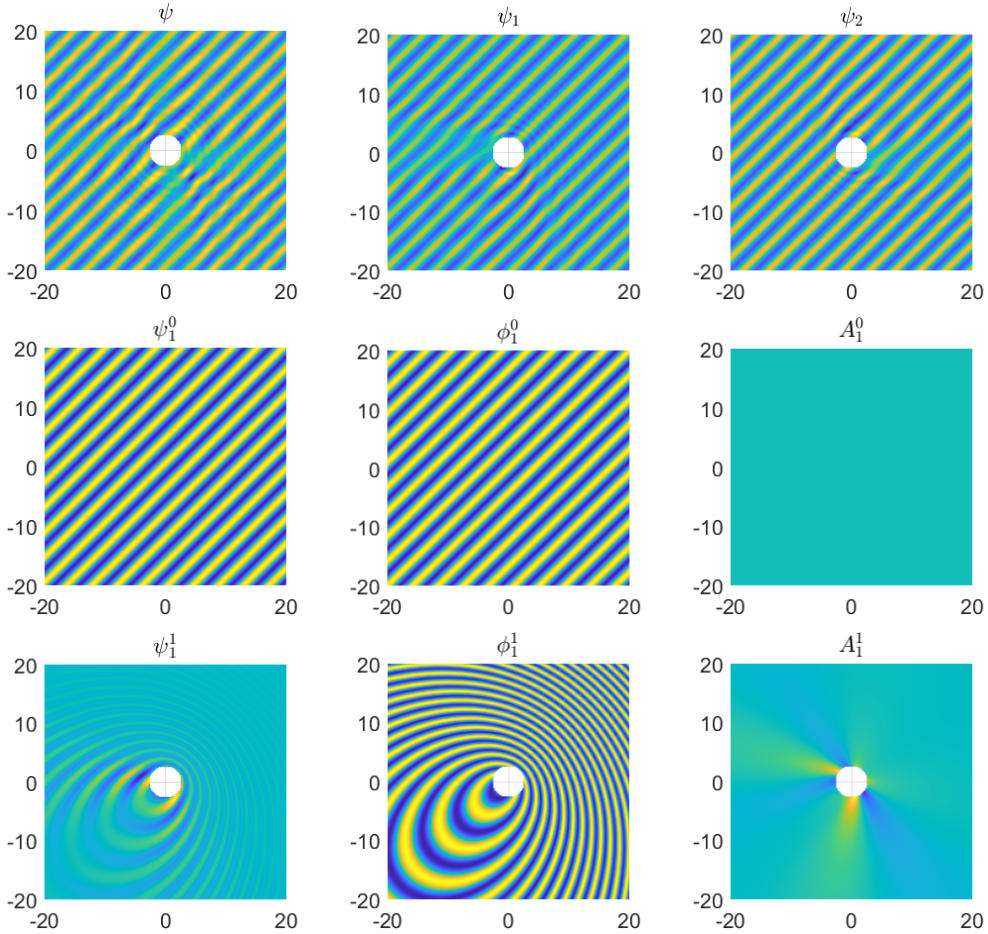

Figure 2: (Top) Visualisation of (left) the far field, and the far field due to scatterers (centre) $j = 1$ and (right) $j = 2$; for $\widehat{\mathbf{d}} = (1, 0, 0)$, $\widehat{\mathbf{x}} = (0, 1, 0)$, $k = 3$. (Middle, Bottom) Visualisation of (15) for $j = 1$: (left) zeroth and first order ψ_1^0 and ψ_1^1; (centre) phase terms ϕ_1^0 and ϕ_1^1; and (right) slowly-varying modulation functions A_1^0 and A_1^1.

modulation functions $A_j^1(\mathbf{c})$ are slowly varying, and therefore amenable to approximation using low-degree tensor-product polynomials.

In summary, combining (11), (13) and (10),

$$\psi_j^1(\mathbf{x}_1,\mathbf{x}_2) = e^{ik\left(\mathbf{x}_{\neq j}\cdot\widehat{\mathbf{d}}+|\mathbf{c}|+\mathbf{x}_j\cdot(-\widehat{\mathbf{x}})\right)} A_j^1(\mathbf{c}), \quad j=1,2. \tag{14}$$

We emphasise that $A_j^1(\mathbf{c})$ is much easier to approximate using low-degree polynomials than $\psi_j^1(\mathbf{x}_1,\mathbf{x}_2)$ because it is dependent on fewer variables, and is slowly varying, whereas $\psi_j^1(\mathbf{x}_1,\mathbf{x}_2)$ is highly oscillatory.

From (6), (8) and (14), the final approximation to the far field is

$$\psi(\mathbf{x}_1,\mathbf{x}_2) \approx \sum_{j=1}^{2} \phi_j^0(\mathbf{x}_j)A_j^0 + \phi_j^1(\mathbf{x}_1,\mathbf{x}_2)\,A_j^1(\mathbf{c}), \quad \mathbf{c}=\mathbf{x}_2-\mathbf{x}_1, \tag{15}$$

$$A_j^0 = \phi_j^0(\mathbf{0}), \quad \phi_j^0(\mathbf{x}_j) = e^{ik\mathbf{x}_j\cdot(\widehat{\mathbf{d}}-\widehat{\mathbf{x}})}, \quad \phi_j^1(\mathbf{x}_1,\mathbf{x}_2) = e^{ik[\mathbf{x}_{\neq j}\cdot\widehat{\mathbf{d}}+|\mathbf{c}|+\mathbf{x}_j\cdot(-\widehat{\mathbf{x}})]}.$$

To setup our surrogate model offline, we compute low degree tensor product polynomials $\tilde{A}_j^1(\mathbf{c})$, approximating $A_j^1(\mathbf{c})$, using a pseudo-spectral method [13], and the required values of $A_j^1(\mathbf{c})$ at the quadrature points are obtained numerically using the T-matrix method. Our surrogate $\tilde{\psi}(\mathbf{x}_1,\mathbf{x}_2)$ is then

$$\psi(\mathbf{x}_1,\mathbf{x}_2) \approx \tilde{\psi}(\mathbf{x}_1,\mathbf{x}_2) = \sum_{j=1}^{2} \phi_j^0(\mathbf{x}_j)A_j^0 + \phi_j^1(\mathbf{x}_1,\mathbf{x}_2)\tilde{A}_j^1(\mathbf{c}), \quad \mathbf{c}=\mathbf{x}_2-\mathbf{x}_1. \tag{16}$$

4 Results

In our numerical experiments we simulate our particle/wave propagation system with frame rate 100 Hz, that is, one frame every 0.01 s for $t \in [0, 10]$ s. In units for distance cm, time s, and mass kg, the acceleration due to gravity is $\mathbf{g} = (0, 0, -980)$, and the attachment point for the strings is $\mathbf{x}_0 = (0, 0, 1000)$. The parameter values for our simulation are listed in Table 1. The initial conditions are

$$\mathbf{x}_1(0) = (-10, 0, 10), \quad \dot{\mathbf{x}}_1(0) = (0, 10, 0),$$

Table 1: Parameter values for the two-particle problem.

	Radius r (cm)	Mass m (kg)	Drag μ	Elastic l	Elastic κ
Particle 1	1.0	3.0e-2	1.0e-3	9.5e2	6.25e-1
Particle 2	1.5	3.6e-2	1.5e-3	9.5e2	7.40e-1

$$x_2(0) = (10, 0, -10)\,, \qquad \dot{x}_2(0) = (0, -10, 0)\,. \tag{17}$$

We simulate the motion of the particles (Figure 1) using the Runge–Kutta 5(4) method in Matlab using the `ode45` function, with both absolute and relative tolerance 1e-6. The wave source is an incident plane wave (3) with direction $\widehat{\mathbf{d}} = (1, 0, 0)$ and wave number $k = 3$.

In Figure 3 we demonstrate the accuracy of our surrogate model by plotting the real part of the far field measured in the four observation directions, $\widehat{\mathbf{x}} = (\pm 1, 0, 0), (0, \pm 1, 0)$. For comparison, we also plot the reference solution computed using the T-matrix-based code [11]. Extensive numerical results by Ganesh and Hawkins [11] establish the accuracy of the reference solution. The surrogate used in Figure 3 has degree 5 tensor product polynomials. The function to be approximated is extremely complicated; it is highly oscillatory but not periodic, and defined over a large domain compared to the period of the oscillations. Such functions are extremely challenging to approximate, especially using low-degree polynomial approximations. The results in Figure 3 show that degree 5 polynomials are able to give visual accuracy to the true far field almost everywhere. Numerical results for higher degree polynomials (not shown) produce substantially higher accuracy. Accuracy can be maintained when the particles are very close together, using a higher truncation parameter in the Born series, at the expense of greater CPU time.

Table 2 presents the CPU times required on an 11th Generation Intel Core i7 machine to solve the ODE (1) for $t = [0, 10]$ to compute the position of the particles at every frame, and then to compute the far field using the T-matrix and the surrogate. In every case the surrogate is more than 600 times faster than the T-matrix code.

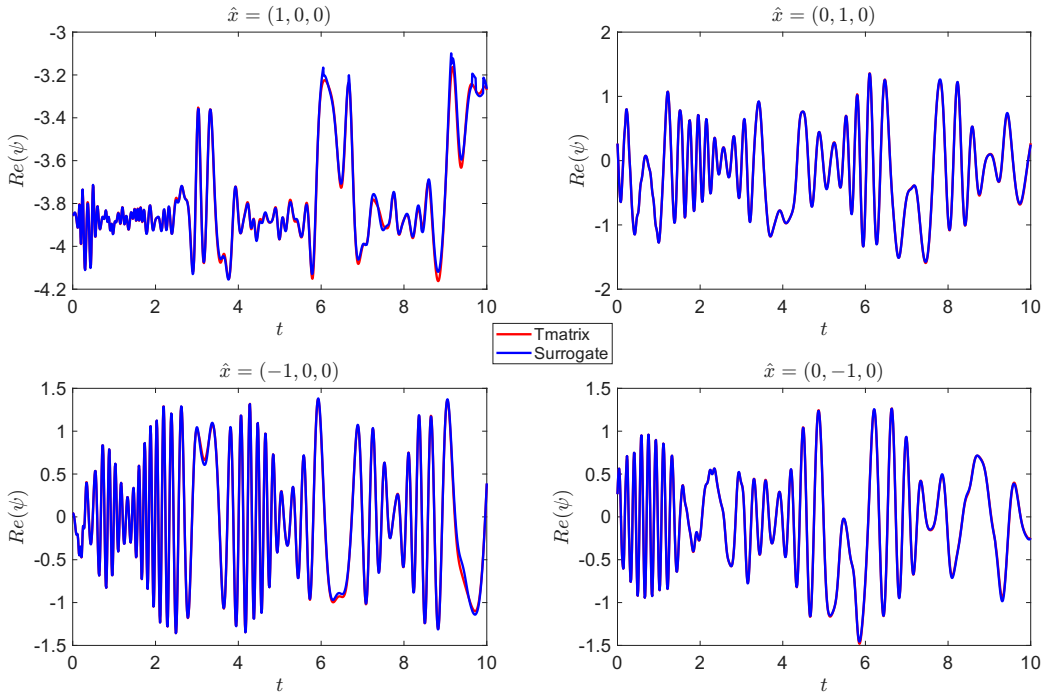

Figure 3: Real part of the far field at four observation directions for plane wave direction $\mathbf{d} = (1, 0, 0)$, obtained from (blue) surrogate degree 5 polynomials and (red) the T-matrix.

Table 2: The ODE is evaluated first for $t \in [0, 10]$ s using the Runge–Kutta 5(4) method, then far field is evaluated at 0.01 s time-steps. CPU times for surrogate polynomials of different degrees are compared to the T-matrix approach.

	Surr. (deg 3)	Surr. (deg 5)	Surr. (deg 7)	T-matrix
Time (s)	0.048980	0.049248	0.051435	33.309841
× faster	680.0703	676.3694	647.6104	-

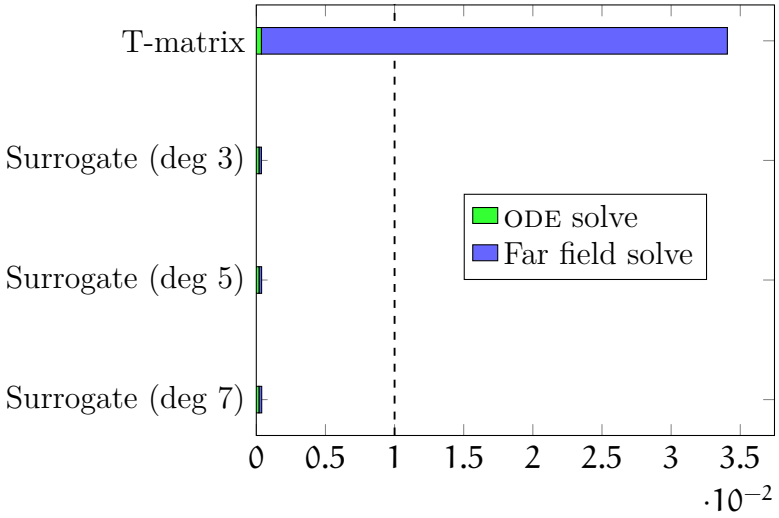

Figure 4: Gantt chart showing CPU times for the ODE solve and subsequent far field evaluation. The 0.01 s frame interval is marked by the dashed line.

Of particular interest is the case where the motion of the particles is directed by the observed wave data. This kind of control problem happens, for example, in a computer game. In this case computing the position of the particles cannot be separated from the wave propagation simulation. Here we solve the ODE to obtain the positions at the new frame from the previous one, and then compute the wave propagation for that frame. Figure 4 shows the amount of time taken for each component of the simulation to compute one frame from the previous one. In this case it is essential that all simulation be completed within the 0.01 s frame rate. This is possible using the surrogate models, but the T-matrix method is too slow, requiring 0.034 s.

References

[1] K. E. Atkinson. *The Numerical Solution of Integral Equations of the Second Kind*. Cambridge Monographs on Applied and Computational

Mathematics. Cambridge University Press, 1997. DOI: 10.1017/CBO9780511626340 (cit. on p. C132).

[2] J. Bruning and Y. Lo. "Multiple scattering of EM waves by spheres part I—Multipole expansion and ray-optical solutions". In: *IEEE Trans. Ant. Prop.* 19.3 (1971), pp. 378–390. DOI: 10.1109/TAP.1971.1139944 (cit. on p. C133).

[3] O. P. Bruno, C. A. Geuzaine, J. A. Monro, and F. Reitich. "Prescribed error tolerances within fixed computational times for scattering problems of arbitrarily high frequency: The convex case". In: *Phil. Trans. A* 362 (2004), pp. 629–645. DOI: 10.1098/rsta.2003.1338 (cit. on p. C132).

[4] S. N. Chandler-Wilde, I. G. Graham, S. Langdon, and E. A. Spence. "Numerical-asymptotic boundary integral methods in high-frequency acoustic scattering". In: *Acta Numer.* 21 (2012), pp. 89–305. DOI: 10.1017/S0962492912000037 (cit. on p. C132).

[5] D. Colton and R. Kress. *Inverse Acoustic and Electromagnetic Scattering Theory*. 4th ed. Applied Mathematical Sciences, 93. Cham: Springer International Publishing, 2019. DOI: 10.1007/978-3-030-30351-8 (cit. on pp. C132, C134, C135, C136).

[6] V. Domínguez, I. G. Graham, and V. P. Smyshlyaev. "A hybrid numerical-asymptotic boundary integral method for high-frequency acoustic scattering". In: *Numer. Math.* 106.3 (2007), pp. 471–510. DOI: 10.1007/s00211-007-0071-4. (Cit. on p. C132).

[7] T. Dufva, J. Sarvas, and J. Sten. "Unified derivation of the translational addition theorems for the spherical scalar and vector wave functions". In: *Prog. Electromagn. Res. B* 4 (2008), pp. 79–99. DOI: 10.2528/PIERB07121203 (cit. on p. C132).

[8] F. Ecevit and F. Reitich. "Analysis of multiple scattering iterations for high-frequency scattering problems. I: the two-dimensional case". In: *Numer. Math.* 114.2 (2009), pp. 271–354. DOI: 10.1007/s00211-009-0249-z. (Cit. on p. C133).

[9] M. Ganesh and I. G. Graham. "A high-order algorithm for obstacle scattering in three dimensions". In: *J. Comput. Phys.* 198.1 (2004), pp. 211–242. DOI: 10.1016/j.jcp.2004.01.007 (cit. on p. C132).

[10] M. Ganesh and S. C. Hawkins. "A fully discrete Galerkin method for high frequency exterior acoustic scattering in three dimensions". In: *J. Comput. Phys.* 230.1 (2011), pp. 104–125. DOI: 10.1016/j.jcp.2010.09.014. (Cit. on p. C132).

[11] M. Ganesh and S. C. Hawkins. "A numerically stable T-matrix method for acoustic scattering by nonspherical particles with large aspect ratios and size parameters". In: *J. Acoust. Soc. Am.* 151.3 (2022), 1978–1988. DOI: 10.1121/10.0009679 (cit. on pp. C132, C135, C140).

[12] C. Geuzaine, O. Bruno, and F. Reitich. "On the O(1) solution of multiple-scattering problems". In: *IEEE Trans. Magnet.* 41 (2005), pp. 1488–1491. DOI: 10.1109/TMAG.2005.844567 (cit. on p. C133).

[13] O. P. Le Maître and O. M. Kino. *Spectral Methods for Uncertainty Quantification*. Springer, 2010. DOI: 10.1007/978-90-481-3520-2 (cit. on p. C139).

[14] P. A. Martin. *Multiple Scattering: Interaction of Time-Harmonic Waves with N Obstacles*. Encyclopedia of Mathematics and its Applications. Cambridge University Press, 2006. DOI: 10.1017/CBO9780511735110 (cit. on p. C132).

[15] P. C. Waterman. "New formulation of acoustic scattering". In: *J. Acoust. Soc. Am.* 45.6 (1969), pp. 1417–1429. DOI: 10.1121/1.1911619 (cit. on p. C132).

Author addresses

1. **M. J. Fernandes**, School of Mathematical and Physical Sciences, Macquarie University, Sydney NSW 2109, AUSTRALIA.
mailto:matthew.fernandes@mq.edu.au
orcid:0009-0003-2421-6834

2. **S. C. Hawkins**, School of Mathematical and Physical Sciences, Macquarie University, Sydney NSW 2109, Australia.
mailto:stuart.hawkins@mq.edu.au
orcid:0000-0003-1642-613X